Title

Removing the Two-Phase Transition in Spinel LiMn2O4 through Cation Disorder

Journal

ACS Energy Letters, 8(1)

ISSN

2380-8195

Authors

Chen, Tina

Yang, Julia

Barroso-Luque, Luis

et al.

Publication Date

2023-01-13

DOI

10.1021/acsenergylett.2c02141

ACS Energy LETTERS

http://pubs.acs.org/journal/aelccp

Removing the Two-Phase Transition in Spinel $LiMn_2O_4$ through Cation Disorder

Tina Chen, Julia Yang, Luis Barroso-Luque, and Gerbrand Ceder*

Cite This: *ACS Energy Lett.* 2023, 8, 314–319

Read Online

ACCESS | Metrics & More | Article Recommendations | Supporting Information

ABSTRACT: **Resource constraints have become critical for the Li-ion industry. Spinel $LiMn_2O_4$ presents a cheaper, more sustainable alternative to traditional layered Li-ion cathodes, but its capacity is constrained by a two-phase transition at 3 V associated with large, inhomogeneous volume change leading to capacity loss. In this Letter, we argue that disorder can replace the two-phase region with solid-solution behavior to create high-capacity cathodes. By investigating the voltage curve and lithiation pathway of $LiMn_2O_4$ spinel with varying levels of Mn disorder, we find that disorder shortens the 3 V plateau by raising the energy landscape and stabilizing motifs found in solid-solution configurations. The plateau disappears completely with 25% Mn 16c occupancy. These results provide guidance on the optimal level of disorder in spinels to achieve both solid-solution behavior and good Li mobility and also highlight more generally how disorder can be utilized to reduce the effects of problematic phase transformations in ordered frameworks.**

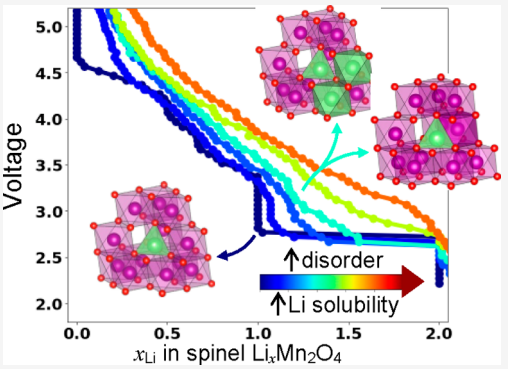

Rechargeable lithium-ion (Li-ion) batteries are used as the energy storage device of choice in electric vehicles.[1] With the increasing electrification of transportation, demand for Li-ion batteries is expected to grow nearly 5-fold in the coming decade.[2] Currently, the Li-ion cathode industry is dominated by well-ordered layered materials, such as Li-(Ni,Mn,Co)O_2 (NMC) and Li(Ni,Co,Al)O_2 (NCA). With their two-dimensional pathways enabling facile Li transport, these layered materials display impressive electrochemical performance but require Co or Ni to remain chemically stable in octahedral environments.[3] As both Co and Ni are expensive and resource-scarce,[4] it is imperative to develop high-energy-density cathodes with alternative structures that can utilize broader chemistries.

One prime example of such an alternative structure is spinel $LiMn_2O_4$, which uses earth-abundant Mn and also has excellent rate capability and thermal stability (of Mn^{4+}) in the charged state.[5−8] While its theoretical capacity is 285 mA h g^{-1}, in commercial use its Li cycling has been restricted to the 4 V range between Mn_2O_4 and $LiMn_2O_4$ which provides only half the theoretical capacity. The remaining capacity cannot be accessed because cycling the additional Li between $LiMn_2O_4$ and $Li_2Mn_2O_4$ occurs at ∼3 V through a strong two-phase reaction.[5,9,10] Such first order transitions proceed with a strong compositional inhomogeneity in cathode particles leading to large stresses and concomitant capacity degradation.[11]

Guided by the general concept that disorder can disrupt the orderings, and thus reduce the strength, of two-phase reactions, recent experiments on heavily ball-milled cation-excess Li−Mn−O−F spinels confirm that disorder can indeed remove the 3 V plateau and lead to a high-rate, high-energy-density cathode material.[12,13] While the most common type of disorder associated with spinel is inversion, in which the 16d transition metals (TM) swap with the 8a cations,[14,15] experiments (in the Li−Mn−O−F systems and a Li-$(Co,Al)_2O_4$ system)[12,13,16] indicate that TM occupancy of the 16c sites is crucial to disrupting the phase transition at the 3 V plateau. Li occupancy of 16d sites has also been shown to enable face-sharing environments seen in solid-solution-like configurations through the phase transition in spinel $Li_4Ti_5O_{12}$.[17,18]

In this paper, we model the complex structural arrangements that occur when a spinel is forced to undergo disorder of the 16d TM onto the 16c sites and investigate its electrochemical voltage profile and lithiation behavior. We demonstrate that even with modest amounts of disorder the solid-solution

Received: September 20, 2022
Accepted: November 28, 2022
Published: December 2, 2022

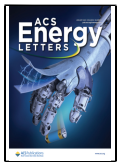

https://doi.org/10.1021/acsenergylett.2c02141
ACS Energy Lett. 2023, 8, 314–319

region of spinel can be extended, leading to a much smaller two-phase region. At larger levels of disorder, the two-phase region can be fully transformed into a solid-solution regime, consistent with experiments, pointing at cathode materials that can combine very high rate with very high capacity.

To investigate the complex configurational space that results with 16c/16d disorder, we build a cluster expansion (CE) model of the configurational energetics of the system, as described in section 1 in the Models and Methods section in the Supporting Information (SI). The model reproduces well the physical properties (i.e., phase diagram) of the DFT training data, as shown in Figure S2 in the SI. This model parametrizes the total energy of configurations in terms of site occupancies on the lattice and, when fitted to the interactions of clusters of sites, can be used in conjunction with Monte Carlo (MC) simulations (as described in the SI Model and Methods, section 2) to enable the calculation of finite-temperature thermodynamics with near ab initio precision. We fit the model to energies of configurations calculated using density functional theory (DFT) and verify the CE's performance against the DFT data using physically relevant properties in the SI Model and Methods, section 3. Using semi-grand-canonical (sgc) MC, we calculate the voltage curves associated with topotactic (de)lithiation within spinel frameworks with varying levels of Mn 16c/16d disorder d from the 16d sites onto the 16c sites, where d indicates the 16c Mn occupancy.

Figure 1 shows the calculated voltage profiles from sgc MC simulations of the disordered spinels, with increasing 16c/16d

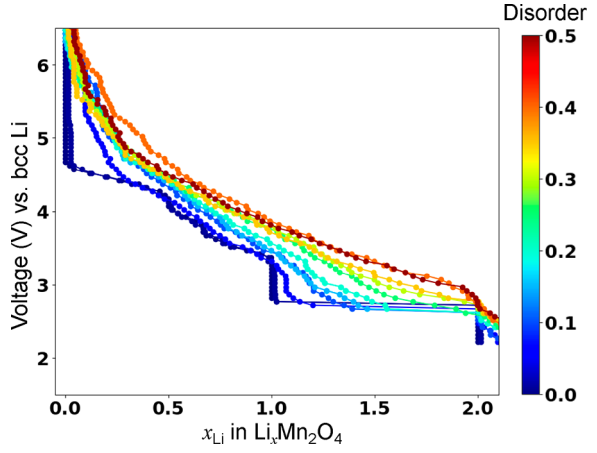

Figure 1. Semi-grand-canonical Monte Carlo-simulated voltage curves of spinel $Li_xMn_2O_4$ with varying levels of Mn disordered from the 16d sites onto the 16c sites from d = 0.0 (ordered spinel, shown in dark blue) to d = 0.5 (fully disordered spinel, shown in dark red).

disorder visualized through color gradation from blue to red. The dark blue curve shows the voltage profile of the ordered spinel phase with d = 0.0, which includes the characteristic spinel plateaus at ~3 V and ~4.3 V. The two-phase region at ~3 V is evident by the large discontinuity in composition (x_{Li}). Compared to experimental results of the ordered spinel $LiMn_2O_4$,[9,19,20] the simulated voltage profile shows more steeply sloped behavior from ~3.8 V to the ~4.3 V plateau due to the self-interaction of Mn in DFT, which is discussed further in SI Note 1. Additional comparisons of the average voltages of lithiation in ordered $LiMn_2O_4$ when using different DFT parameters (Li pseudopotential and DFT functional) are shown in Figures S1 and S3, and an additional comparison to the Monte Carlo simulation is shown in Figure S4. An additional small voltage step is also seen at around x = 0.7, which is consistent with experiments at temperatures slightly below room temperature.[21]

As the Mn disorder onto the 16c sites increases, the ~3 V plateau shortens starting from d = 0.05 and completely disappears when d = 0.25. The shortening of the ~3 V plateau is a result of increased solubility on the x_{Li} = 1.0 side. The ~4.3 V plateau also disappears, and the more complex behavior around x_{Li} = 0.5 is replaced with linearly sloping behavior. This is consistent with previous studies in $Li_{1+x}Mn_{2-x}O_4$ showing that the step at x_{Li} = 0.5 in $LiMn_2O_4$ can be smoothed out by cation disorder on the 16d sites, as it originates mainly from interactions between 8a tetrahedral Li.[22] The steeply sloping behavior of the highly disordered spinels is also consistent with that of the disordered rocksalts,[23] which the disordered spinels approach when the Mn are fully disordered over the 16c and 16d octahedral sites ($d \rightarrow 0.5$). The higher voltages as $x_{Li} \rightarrow 0$ for more disordered spinels, however, are not consistent and due to the lack of oxygen oxidation, which is not included as a redox mechanism in the CE model. Explicit DFT calculations in this regime, in which oxygen oxidation is allowed, are consistent with experiments on the partially disordered spinel, as described in SI Note 2 and shown in Figures S5 and S6. An overall increase in average voltage with disorder can also be observed, indicating that disorder raises the energy of the fully delithiated Mn_2O_4 more so than it does the fully lithiated $Li_2Mn_2O_4$.[24,25]

We hypothesize that the mechanism by which 16c/16d disorder removes the two-phase region is through raising the energies of the stable phases (spinel $LiMn_2O_4$ and lithiated spinel $Li_2Mn_2O_4$) and lowering the energies of the solid-solution configurations at intermediate Li composition. Disorder on 16c/16d increases the energy of the spinel phase because electrostatic repulsion when Mn occupies 16c raises the site energy of Li in the face-sharing 8a sites. Disorder on 16c/16d can also lower the energy of the solid-solution phase through Li occupancy of non-Mn-occupied 16d sites, which stabilizes face-sharing environments in spinel $Li_4Ti_5O_{12}$.[17,18] Using the CE and MC simulations, we confirm our hypothesis and obtain an additional mechanistic understanding by sampling the configurations observed along the phase transition.

To confirm that the energies of the spinel and lithiated spinel increase with the addition of 16c/16d disorder, we use the CE to evaluate the configurational energies of 100 partially disordered configurations, generated as described in SI Note 3, at the compositions $LiMn_2O_4$ and $Li_2Mn_2O_4$. The energies of partially disordered $LiMn_2O_4$ (green) and $Li_2Mn_2O_4$ (red) are shown with respect to the ordered states in Figure 2. Both spinel and lithiated spinel energies increase with disorder, but the energy increase is most pronounced for the $LiMn_2O_4$ spinel due to the decrease in tetrahedral Li in $LiMn_2O_4$ with disorder (see Figure S7 in the SI). Thus, Figure 2 confirms that the endmember phases of the two-phase region in ordered spinel become less stable with disorder, but the effect is more pronounced in $LiMn_2O_4$.

To investigate how disorder stabilizes solid-solution configurations relative to the spinel and lithiated spinel, we analyze the configurations sampled by the MC within the x_{Li} range of the two-phase region to understand how (de)-

https://doi.org/10.1021/acsenergylett.2c02141
ACS Energy Lett. 2023, 8, 314−319

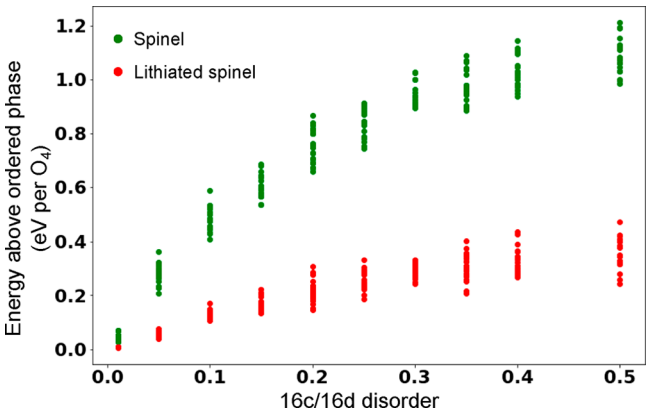

Figure 2. CE-calculated energies associated with disordering an increasing number of 16d Mn in spinel $LiMn_2O_4$ (red) and lithiated spinel $Li_2Mn_2O_4$ (green) onto the 16c sites. Energies are calculated with respect to the ordered spinel (for the disordered spinels) and the ordered lithiated spinel (for the disordered lithiated spinels).

lithiation occurs in the partially disordered spinel compared to the ordered spinel. Figure 3 shows the concentration of tetrahedral (tet) and octahedral (oct) Li environments (Figure 3a,b) and tet environments categorized by the presence of any face-sharing nearest neighbor cations (Figure 3c,d) in the ordered (d = 0.0) system and a disordered (d = 0.1) system. The concentrations of tet-occupied and oct-occupied Li are shown in green and red in Figure 3a,b, and the isolated (non-face-sharing) tet Li, Li-face-shared tet Li, Mn-face-shared tet Li, and both Li- and Mn-face-shared tet Li are shown in black, blue, purple, and orange, respectively, in Figure 3c,d.

The results in Figure 3a,c confirm that, in the ordered system (d = 0.0), Li is inserted into isolated tet sites (8a sites, left inset in Figure 3c) until they are fully occupied (transparent green regime). The sudden jump in x_{Li} indicates a phase transition (transparent blue regime) along with the shift from tet to oct occupancy (right inset in Figure 3c). Lithiation in the disordered system (d = 0.1) initially proceeds as in the ordered system, with the insertion of isolated tet Li. From $x_{Li} \approx 0.4$ to $x_{Li} \approx 1.2$, Li begins to occupy oct sites (left inset in Figure 3d), as evidenced by the rise in oct Li concentration (red in Figure 3b), and Mn-face-sharing tet sites (right inset in Figure 3d), as evidenced by the rise in tet Li with Mn-face-sharing environments (purple in Figure 3d). While the lower electrostatics between face-sharing Li_{tet} and Li_{oct} than between face-sharing Li_{tet} and Mn_{oct} would suggest a predominance of Li−Li face-sharing over Li−Mn face-sharing, the vastly larger population of tetrahedral environments that have a singly face-sharing Mn compared to those face-sharing with only one Li (see Figure S8 in the SI) makes it more likely for Li to be inserted into Mn-face-sharing sites, creating the

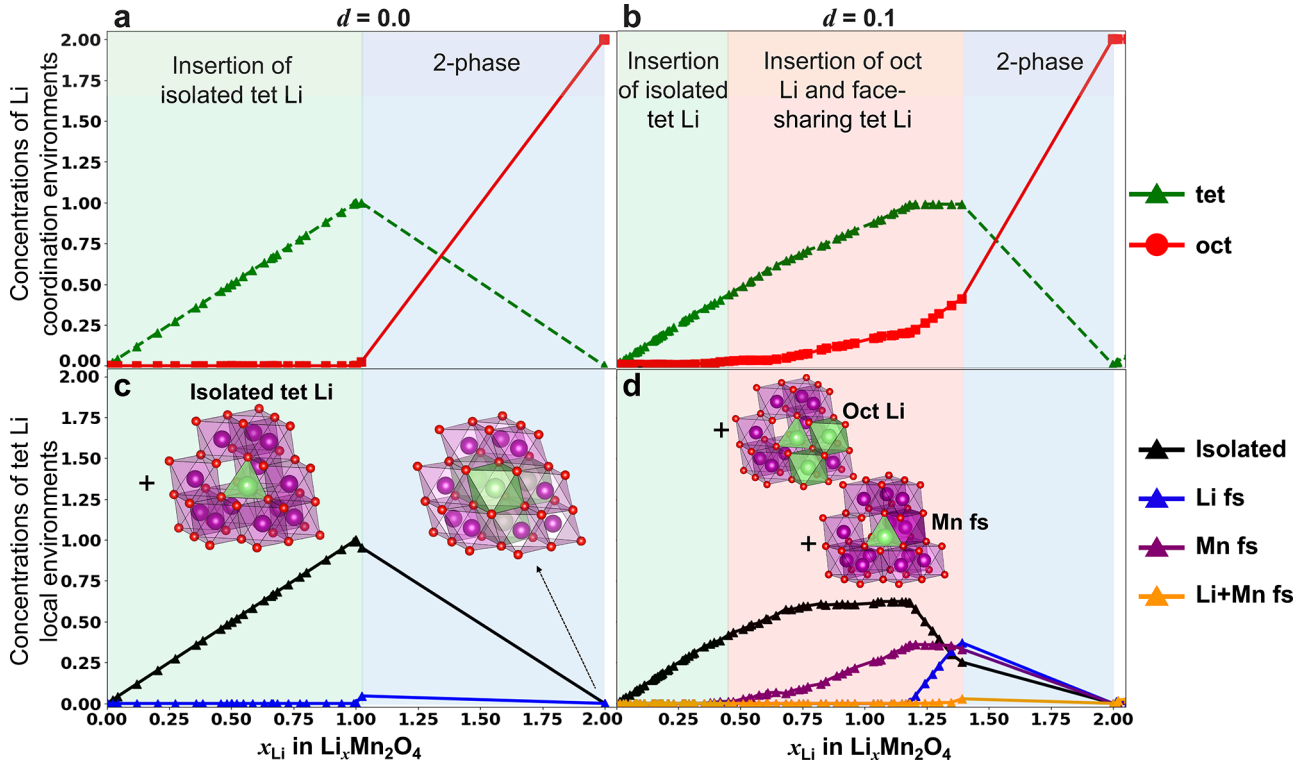

Figure 3. Averaged concentrations (per O_4) of Li in tet (green triangles) and oct (red circles) coordination environments for the ordered spinel with d = 0.0 (a) and the slightly disordered spinel with d = 0.1 (b); and averaged concentrations of tet Li categorized by the species in their face-sharing nearest neighbor oct sites, including isolated with no face-sharing (black triangles), face-sharing with Li (blue), face-sharing with Mn (purple), and face-sharing with both Li and Mn (orange) in the ordered spinel (c) and the slightly disordered spinel (d). Lithiation is split into regimes based on the type of environment Li is inserted, beginning with the insertion of isolated tet Li (transparent green), followed by the insertion of oct Li and face-sharing tet Li (transparent red), and ending in a two-phase region between a spinel-like phase and the lithiated spinel (in which all Li occupy the non-Mn-occupied oct sites, transparent blue). Insets show examples of local Li environments, such as isolated tet Li inserted during the green regime of lithiation in panel c, the fully lithiated spinel's oct Li in panel c, and oct Li and face-sharing tet Li inserted during the red regime in panel d.

https://doi.org/10.1021/acsenergylett.2c02141
ACS Energy Lett. 2023, 8, 314−319

face-sharing Li−Mn seen in Figure 3d. Besides a flattening of the isolated tet occupancy, no particular change in site occupancies characterizes the typical $LiMn_2O_4$ spinel stoichiometry even for this moderate level of disorder. Instead, lithiation until $x_{Li} \approx 1.4$ involves Li occupying Li-face-sharing tet sites (blue in Figure 3d). The regime involving more complex solid-solution insertion of Li into oct sites and face-sharing tet sites is highlighted in transparent red. The two-phase region in the $d = 0.1$ disordered spinel is already significantly reduced and appears between $x_{Li} \approx 1.4$ and $x_{Li} \approx 2.0$.

At intermediate Li content, face-sharing tet sites and oct sites in the disordered system are not accessible in the ordered spinel but are energetically competitive enough to appear in the disordered system. Unlike the only doubly face-sharing oct environments available in the ordered spinel, the disordered system contains environments with only one face-sharing contact, creating less electrostatic repulsion. The additional occupation of oct sites and face-sharing tet sites allows solid-solution insertion of Li past the spinel composition ($x_{Li} = 1.0$) to $x_{Li} \approx 1.4$, shortening the two-phase region and voltage plateau from 1.0 Li/Mn_2O_4 to 0.6 Li/Mn_2O_4.

From the configurational energies of the disordered spinel and lithiated spinel (Figure 2) and the configurations sampled from MC (Figure 3), we find that disorder reduces the two-phase region by destabilizing the spinel and lithiated spinel phases and stabilizing solid-solution configurations. These two effects can be clearly observed in Figure 4 which shows the

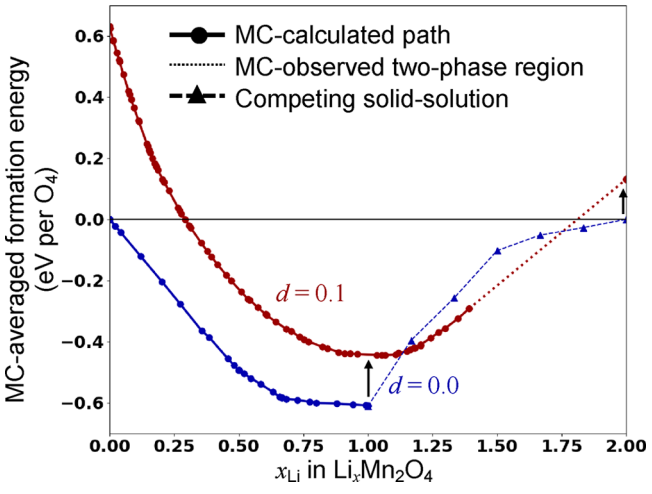

Figure 4. Averaged formation energies of sampled configurations from topotactic (de)lithiation of $Li_xMn_2O_4$ with sgc MC for the $d = 0.0$ ordered spinel (blue) and the $d = 0.1$ disordered spinel (maroon), with two-phase regions observed by the MC displayed as dotted lines. The dashed blue line signifies the solid-solution pathway in the ordered system.

MC-averaged energies for the ordered (blue) and partially disordered ($d = 0.1$, maroon) systems and the lowest CE-energy solid-solution configurations sampled across the phase transition of the ordered system as described in SI Note 4. The energies of all sampled solid-solution configurations are shown in Figure S9. Whereas for the ordered spinel the energy of sampled solid-solution configurations (dashed blue) turns concavely downward for $x_{Li} > 1.0$ due to the high energy of creating face-sharing cation interstitials in the ordered spinel, the partially disordered material allows for significantly more solid solubility past $x_{Li} = 1.0$. Between $x_{Li} = 1.0$ and $x_{Li} = 1.4$ these solid-solution configurations are stabilized by disorder compared to the solid-solution configurations sampled in the ordered phase (dashed blue). A second, more general effect, already highlighted in Figure 2 is the general energy increase of the $LiMn_2O_4$ and $Li_2Mn_2O_4$ compositions (black arrows) which are raised with respect to the intermediate solid-solution compositions. The net effect of these changes in the energy of the system is a shortened two-phase region in the partially disordered system (dotted maroon).

The simulated voltage curves indicate that the two-phase region and ∼3 V voltage plateau disappear at $d = 0.25$, corresponding to 25% Mn 16c occupancy. Spinels with higher levels of disorder also lack two-phase behavior, indicating that they would also display solid-solution behavior, but their spinel characteristics decrease with disorder. Because the Mn begin to occupy 16c sites, the 8a−16c network that enables 3-D Li migration in spinel $LiMn_2O_4$ becomes increasingly obstructed with disorder. While Li can percolate through other tet sites (8b and 48f) that become accessible by disorder,[26] the excess loss of spinel character and its channels with facile Li migration impacts the overall Li mobility in, and thus the rate capability of, the highly disordered materials.[12] Therefore, we suggest that partially disordered spinels should not exceed a level of disorder above $d = 0.25$.

However, disordered spinels with slightly lower levels of disorder ($d = 0.15$−0.20) likely still maintain many of the advantages of the more disordered spinels. For example, disordered spinels with $d = 0.15$−0.20 show significantly shorter voltage plateaus (from $x_{Li} \approx 1.7$ to $x_{Li} \approx 2.0$ per O_4) compared to the ordered spinel ($x_{Li} = 1.0$ to $x_{Li} = 2.0$). Thus, most of the Li inserted through a two-phase region in the ordered spinel can lithiate through solid solution in the $d = 0.15$−0.20 disordered spinels. Such lithiation through solid solution rather than two-phase behavior is expected to be more facile, as the system does not need to overcome barriers associated with nucleation and growth of a secondary phase. Disorder over 16c/16d sites also breaks the 16d Mn ordering that is responsible for the collective Jahn−Teller distortion[27] in the ordered spinel. Thus, partially disordered spinels with 15−20% 16c Mn or TM occupancy are likely to show mostly solid-solution behavior without collective Jahn−Teller distortion as well as good rate capability due to high spinel character.

Our work shows that it may be possible to create a high-capacity earth-abundant spinel cathode material using partial 16c/16d disorder. Using ab initio modeling, we find that Mn disorder between the 16d and 16c sites in spinel $LiMn_2O_4$ shortens the two-phase region and 3 V plateau between $LiMn_2O_4$ and $Li_2Mn_2O_4$, even eliminating it with 25% Mn 16c occupancy. Our analysis indicates that the shortened plateau is due to disorder elevating the overall energy landscape and making higher-energy solid-solution configurations more accessible. The use of disorder to reduce and even remove two-phase regions by raising the overall energy landscape can be extended to other systems with problematic phase transformations within ordered frameworks. The suppression of the rate- and cyclability-limiting two-phase region of the spinel through disorder provides an avenue by which to optimize partially disordered spinels, bringing us another step closer to cheaper high-rate, energy-dense Li-ion cathodes.

https://doi.org/10.1021/acsenergylett.2c02141
ACS Energy Lett. 2023, 8, 314−319

■ ASSOCIATED CONTENT

Supporting Information

The Supporting Information is available free of charge at https://pubs.acs.org/doi/10.1021/acsenergylett.2c02141.

Model and methods; details on the discrepancy between the experimental and simulated voltage curves of the ordered spinel $LiMn_2O_4$; analysis on the effect of oxygen oxidation on the disordered spinel voltage curves; details on the generation of the disordered $LiMn_2O_4$ and $Li_2Mn_2O_4$; details on sampling of the solid-solution configurations in the two-phase region of the ordered system; and analysis between cluster expansion-evaluated energy of disordered $LiMn_2O_4$ configurations and fraction of tetrahedral Li (PDF)

■ AUTHOR INFORMATION

Corresponding Author

Gerbrand Ceder − *Department of Materials Science and Engineering, University of California Berkeley, Berkeley, California 94720, United States; Materials Sciences Division, Lawrence Berkeley National Laboratory, Berkeley, California 94720, United States;* orcid.org/0000-0001-9275-3605; Email: gceder@berkeley.edu

Authors

Tina Chen − *Department of Materials Science and Engineering, University of California Berkeley, Berkeley, California 94720, United States; Materials Sciences Division, Lawrence Berkeley National Laboratory, Berkeley, California 94720, United States;* orcid.org/0000-0003-0254-8339

Julia Yang − *Department of Materials Science and Engineering, University of California Berkeley, Berkeley, California 94720, United States; Materials Sciences Division, Lawrence Berkeley National Laboratory, Berkeley, California 94720, United States*

Luis Barroso-Luque − *Department of Materials Science and Engineering, University of California Berkeley, Berkeley, California 94720, United States; Materials Sciences Division, Lawrence Berkeley National Laboratory, Berkeley, California 94720, United States;* orcid.org/0000-0002-6453-9545

Complete contact information is available at: https://pubs.acs.org/10.1021/acsenergylett.2c02141

Author Contributions

G.C. conceived and supervised the project. T.C. built the model, performed the computations and analysis, and wrote the manuscript. J.Y. and L.B.-L. developed and implemented the methods to fit the model and perform the Monte Carlo calculations. All authors discussed, reviewed, and edited the manuscript.

Notes

The authors declare no competing financial interest.

■ ACKNOWLEDGMENTS

Financial support is acknowledged from the Assistant Secretary for Energy Efficiency and Renewable Energy, Vehicle Technologies Office, under the Applied Battery Materials Program, of the U.S. Department of Energy (DOE) under Contract No. DE-AC02-05CH11231. The research was performed using computational resources sponsored by the DOE Office of Energy Efficiency and Renewable Energy and located at the National Renewable Energy Laboratory and from the Center for Functional Nanomaterials (CFN), which is a U.S. DOE Office of Science User Facility, at Brookhaven National Laboratory under Contract No. DE-SC0012704.

■ REFERENCES

(1) Olivetti, E. A.; Ceder, G.; Gaustad, G. G.; Fu, X. Lithium-Ion Battery Supply Chain Considerations: Analysis of Potential Bottlenecks in Critical Metals. *Joule* **2017**, *1* (2), 229−243.

(2) Zhou, Y.; Gohlke, D.; Rush, L.; Kelly, J.; Dai, Q. *Lithium-Ion Battery Supply Chain for E-Drive Vehicles in the United States: 2010−2020*; ANL/ESD-21/3; 167369; Argonne National Lab. (ANL): Argonne, IL, 2021.

(3) Reed, J.; Ceder, G. Role of Electronic Structure in the Susceptibility of Metastable Transition-Metal Oxide Structures to Transformation. *Chem. Rev.* **2004**, *104* (10), 4513−4534.

(4) Clément, R.; Lun, Z.; Ceder, G. Cation-Disordered Rocksalt Transition Metal Oxides and Oxyfluorides for High Energy Lithium-Ion Cathodes. *Energy Environ. Sci.* **2020**, *13* (2), 345−373.

(5) Thackeray, M.; David, W.; Bruce, P.; Goodenough, J. Lithium Insertion into Manganese Spinels. *Mater. Res. Bull.* **1983**, *18* (4), 461−472.

(6) Thackeray, M. M. Manganese Oxides for Lithium Batteries. *Prog. Solid State Chem.* **1997**, *25* (1−2), 1−71.

(7) Luo, J.-y.; Wang, Y.-g.; Xiong, H.-m.; Xia, Y.-y. Ordered Mesoporous Spinel $LiMn_2O_4$ by a Soft-Chemical Process as a Cathode Material for Lithium-Ion Batteries. *Chem. Mater.* **2007**, *19* (19), 4791−4795.

(8) Shaju, K. M.; Bruce, P. G. A Stoichiometric Nano-$LiMn_2O_4$ Spinel Electrode Exhibiting High Power and Stable Cycling. *Chem. Mater.* **2008**, *20* (17), 5557−5562.

(9) Thackeray, M.; De Kock, A.; Rossouw, M.; Liles, D.; Bittihn, R.; Hoge, D. Spinel Electrodes from the Li-Mn-O System for Rechargeable Lithium Battery Applications. *J. Electrochem. Soc.* **1992**, *139* (2), 363.

(10) Barker, J.; Koksbang, R.; Saidi, M. Y. Lithium Insertion in Manganese Oxides: A Model Lithium Ion System. *Solid State Ionics* **1995**, *82* (3−4), 143−151.

(11) Luo, F.; Wei, C.; Zhang, C.; Gao, H.; Niu, J.; Ma, W.; Peng, Z.; Bai, Y.; Zhang, Z. Operando X-Ray Diffraction Analysis of the Degradation Mechanisms of a Spinel $LiMn_2O_4$ Cathode in Different Voltage Windows. *J. Energy Chem.* **2020**, *44*, 138−146.

(12) Cai, Z.; Ji, H.; Ha, Y.; Liu, J.; Kwon, D.-H.; Zhang, Y.; Urban, A.; Foley, E. E.; Giovine, R.; Kim, H. Realizing Continuous Cation Order-to-Disorder Tuning in a Class of High-Energy Spinel-Type Li-Ion Cathodes. *Matter* **2021**, *4* (12), 3897−3916.

(13) Ji, H.; Wu, J.; Cai, Z.; Liu, J.; Kwon, D.-H.; Kim, H.; Urban, A.; Papp, J. K.; Foley, E.; Tian, Y. Ultrahigh Power and Energy Density in Partially Ordered Lithium-Ion Cathode Materials. *Nat. Energy* **2020**, *5* (3), 213−221.

(14) Barth, T. F.; Posnjak, E. Spinel Structures: With and without Variate Atom Equipoints. *Z. Kristallogr. - Cryst. Mater.* **1932**, *82* (1−6), 325−341.

(15) Seko, A.; Yuge, K.; Oba, F.; Kuwabara, A.; Tanaka, I. Prediction of Ground-State Structures and Order-Disorder Phase Transitions in II-III Spinel Oxides: A Combined Cluster-Expansion Method and First-Principles Study. *Phys. Rev. B* **2006**, *73* (18), 184117.

(16) Lee, E.; Kwon, B. J.; Dogan, F.; Ren, Y.; Croy, J. R.; Thackeray, M. M. Lithiated Spinel $LiCo_{1-x}Al_xO_2$ as a Stable Zero-Strain Cathode. *ACS Appl. Energy Mater.* **2019**, *2* (9), 6170−6175.

(17) Ganapathy, S.; Vasileiadis, A.; Heringa, J. R.; Wagemaker, M. The Fine Line between a Two-Phase and Solid-Solution Phase Transformation and Highly Mobile Phase Interfaces in Spinel $Li_{4+x}Ti_5O_{12}$. *Adv. Energy Mater.* **2017**, *7* (9), 1601781.

(18) Zhang, W.; Seo, D.-H.; Chen, T.; Wu, L.; Topsakal, M.; Zhu, Y.; Lu, D.; Ceder, G.; Wang, F. Kinetic Pathways of Ionic Transport in Fast-Charging Lithium Titanate. *Science* **2020**, *367* (6481), 1030−1034.

(19) Ohzuku, T.; Kitagawa, M.; Hirai, T. Electrochemistry of Manganese Dioxide in Lithium Nonaqueous Cell: III. X-Ray Diffractional Study on the Reduction of Spinel-Related Manganese Dioxide. *J. Electrochem. Soc.* **1990**, *137* (3), 769.
(20) Goodenough, J. B.; Park, K.-S. The Li-Ion Rechargeable Battery: A Perspective. *J. Am. Chem. Soc.* **2013**, *135* (4), 1167−1176.
(21) Abiko, H.; Hibino, M.; Kudo, T. Temperature Dependence of the Potential-Composition Profiles of $Li_xMn_2O_4$ Spinel. *Electrochem. Solid-State Lett.* **1999**, *1* (3), 114.
(22) Gao, Y.; Reimers, J.; Dahn, J. Changes in the Voltage Profile of $Li/Li_{1+x}Mn_{2-x}O_4$ Cells as a Function of *x*. *Phys. Rev. B* **1996**, *54* (6), 3878.
(23) Lun, Z.; Ouyang, B.; Cai, Z.; Clément, R. J.; Kwon, D.-H.; Huang, J.; Papp, J. K.; Balasubramanian, M.; Tian, Y.; McCloskey, B. D. Design Principles for High-Capacity Mn-Based Cation-Disordered Rocksalt Cathodes. *Chem.* **2020**, *6* (1), 153−168.
(24) Abdellahi, A.; Urban, A.; Dacek, S.; Ceder, G. The Effect of Cation Disorder on the Average Li Intercalation Voltage of Transition-Metal Oxides. *Chem. Mater.* **2016**, *28* (11), 3659−3665.
(25) Yahia, M. B.; Lemoigno, F.; Rousse, G.; Boucher, F.; Tarascon, J.-M.; Doublet, M.-L. Origin of the 3.6 to 3.9 V Voltage Increase in the $LiFeSO_4F$ Cathodes for Li-Ion Batteries. *Energy Environ. Sci.* **2012**, *5* (11), 9584−9594.
(26) Yang, J.; Ceder, G. Activated Internetwork Pathways in Partially-Disordered Spinel Cathode Materials with Ultrahigh Rate Performance. *Adv. Energy Mater.* **2022**, in press.
(27) Ohzuku, T.; Kato, J.; Sawai, K.; Hirai, T. Electrochemistry of Manganese Dioxide in Lithium Nonaqueous Cells: IV. Jahn-Teller Deformation of In. *J. Electrochem. Soc.* **1991**, *138* (9), 2556.

https://doi.org/10.1021/acsenergylett.2c02141
ACS Energy Lett. 2023, 8, 314−319